Hindawi
Journal of Nanomaterials
Volume 2022, Article ID 4647759, 16 pages
https://doi.org/10.1155/2022/4647759

Research Article

An Experimental Assessment into the Pressure and Thermal Efficacy of Chemically Synthesized Nanofluids in Computer Cooling Applications

M. Anish,[1] **P. Bency**,[2] **V. Jayaprakash**,[1] **J. Jayaprabakar**,[1] **Nivin Joy**,[1] **S. K. Sahaya Susmi**,[1] **and T. Arunkumar**[3]

[1]*School of Mechanical Engineering, Sathyabama Institute of Science and Technology, Jeppiar Nagar, Chennai, India*
[2]*Department of Electrical and Electronics Engineering, SRM Valliammai Engineering College, Chennai, India*
[3]*Department of Mechanical Engineering, CMR Institute of Technology, Bengaluru, India*

Correspondence should be addressed to M. Anish; anish.2010me@gmail.com

Received 10 May 2022; Revised 26 July 2022; Accepted 22 September 2022; Published 11 November 2022

Academic Editor: Rajeshkumar Shanmugam

In order to maintain ideal working conditions by reducing heat from the system, a certain mechanism must be put into place. This research aims to investigate the effects of nanofluids on the performance of microchannel heating components used in computer cooling methods. The mixture of 25% ethylene glycol and 75% alkaline water is used to create the working fluids in the experiment. The combination contains nanoparticles of SiC, TiO_2, and ZnO. It is between 25 and 40°C, includes 0.25%–1.5% nanoparticles, and has a volume flow rate of 0.025–0.080 kg/s. The temperature of the central processing unit, the rate of heat transfer, pressure losses, and pumping power have all been researched in relation to the thermal properties of nanofluids and base fluids. Data show that SiC–EG/AW at 1.5% concentration and 0.080 kg/s has a 31% higher coefficient of heat transfer than the base fluid and a temperature that is 9% lower than that of the other nanofluids. This is due to the fact that SiC–EG/AW has the highest pumping force power and TiO_2–EG/AW has the lowest pressure decrease. Because the nanofluid performs better than the basic fluid at cooling computers, a little boost in pumping force and pressure reduction may be acceptable.

1. Introduction

Modern computers generate a lot of heat while they are in operation, which is a serious concern. The technique of transporting and removing heat generated by computer components from a computer system is known as computer cooling. Given that various computer components generate a significant amount of heat when operating, a mechanism for removing this heat should be given so that the computer may work in a safe environment. This is accomplished by the use of computer coolers and the use of appropriate operating fluids [1]. They will also make a huge impact on the system's ability to cool down much quicker as a result of their efforts. Using fluid heat sinks, a huge number of chips may be cooled at the same time. They have the ability to simultaneously cool the central processor, central processing unit (CPU), graphics card, and processor stockpile circuits. The usage of this product has given hope to many computer users who have been looking for a trustworthy and integrated cooler for their computer's internal components. Flowing heat sinks have the potential to cool a chip down to the temperature of the working fluid in the absence of a working fluid. Because of their modest operating flow rates, these heat sinks generate a comparably low level of noise while in operation. Furthermore, when the blower is used in the radiator, the amount of noise created by the system is kept to a bare minimum (of the heat sink) [2]. Heat fluxes generated by electronic equipment, such as LEDs and high-power processors, have grown enormously over the last 2 decades, resulting in the need to remove heat from the semiconductor junctions. A microchannel heat sink (MCHS), which was initially proposed by Tuckerman and Pease [3], has been developed as a novel method of eliminating huge volumes of heat from tiny spaces. This was proven to be the case as a

result of the inverse connection between the peculiar channel length and the coefficient of heat transfer. There are microchannels that allow cooling fluid to flow through the device's highly reactive materials such as aluminum gray metallic alloy, silicone, and copper. According to Tiwari et al. [4], an MCHS also has a number of cooling benefits, including the fact that it is compact and light, that it has a high coefficient of heat transfer, and that it has the aptness to reduce the heat gain of the device under examination, among other things. The development of compact gadgets is dependent on the successful implementation of heat management solutions for modern electrical equipment. These devices must be lightweight and compact in order to provide great performance while being lightweight and compact in size. MCHS provides a solution that has the potential to alleviate heat dissipation issues that are currently being encountered in emerging applications. The MCHS is a piece of hardware that may be used to keep the CPU cool while it is running. As a result, in recent years, MCHS has attracted a great deal of interest from academics and researchers.

Nanofluids are indeed a homogenous combination of nanoparticles and base fluids that may be used for a variety of purposes, including biomedical research. Nanoparticles having average diameters of less than 100 nm may be suspended in a variety of typical heat transfer mediums, including water, oil, ethylene glycol, and others [5]. Choi and Eastman [6] recent research has demonstrated that nanofluids have greater heating characteristics than regular fluids in a range of circumstances and applications. Nanofluids, which are minuscule particles on the nanoscale (usually less than 100 nm in size) suspended in liquids, have surfaced as a prospective contender for consideration in heat transfer systems. Nanofluids are a novel kind of chemical material that has the potential to be used in nanotechnology. Over the past decade, they have received a lot of attention, and they have made significant contributions to improving the heat conductivity of thermal transmitter fluids as well as other fields of research. Rafati et al. [7] discovered that the thermal performance of alumina nanofluid in CPU cooling was outstanding at varied Reynolds numbers. In their investigation of a commercial heat sink for cooling CPU using water and CuO nanofluids. Korpyś et al. [8] assessed the strategy's efficacy using both simulation and hardware methods. Jeng and Teng [9] assessed that a hybrid cooling system for electronic chips that leveraged Al_2O_3/water nanofluid instead of pure water had improved heat dissipation, higher water pump power consumption, and a lower heater surface temperature than a system that used distilled water. According to Yousefi et al. [10], 0.5% Al_2O_3 nanoparticles mixed into the water coolant before use may reduce the thermal resistance of a heat pipe. When nanofluid was present, thermal resistance decreased by 15% at 10 W and by 22% at 25 W, as the temperature increased. Selvakumar and Suresh [11] identified an electronic heat sink with a 0.2% volume fraction of CuO/water nanofluid that improved convective performance by 29.99%. Said et al. [12] stated that the addition, the parametric analysis is carried out to calculate the organic Rankine cycles (ORC) performance in terms of its energetic and exergetic capabilities at a variety of nanoparticle concentrations and volume flow rates. Kumar et al. [13], a research of zeta potential, indicated that cetyltrimethylammonium bromide (CTAB) surfactant has the highest impact up to 30 days after preparation, but sodium dodecylbenzene sulfonate (SDBS) surfactant has the greatest stability beyond 30 days using a 3 : 2 mixing ratio and 90 min of sonication. Stabilization was demonstrated to have an effect on the thermal conductivity of nanofluid hybrids. At temperatures ranging from 25 to 50°C, thermophysical characteristics of hybrid nanofluids were investigated and quantified. When the parameters were changed, values for the thermal conductivity ratios, specific heat, dynamic viscosity ratio, and density were all found to change. The CeO_2–MWCNT–water hybrid nanofluid demonstrated the greatest level of effectiveness, with outstanding thermophysical characteristics and the highest Mouromtseff number (M_O) [14].

For example, Khonsue [15] investigated the cooling performance of an aluminum-based MCHS in an experimental setting. The microchannel's measurements were 40 mm in width, 28 mm in length, and 2 mm in base thickness, respectively. Demonized water was used as the primary fluid in this experiment. Researchers noticed that channels may be expected to rise in height as well as the speed at which water flowed increased the rate of heat transfer. Tran et al. [16] used both experimental and computational methods to examine the pressure gradient of an aluminum MCHS. It was revealed that the mass ratios were between 0.2 and 0.4 g/s, with the input water temperature being 25°C. According to the data, as the rate of mass flow increases, the pressure decreases. In an experimental scenario, Ma et al. [17] examined the heat transmission and the fluid flow via a four-port heat source that included both chevron and rectangular motifs. When the input temperature was equal to 25°C, the flow rate of deionized water varied between 28 and 72 mL/min. Initially, the flow rate-dependent pressure difference in the zigzag microchannel is somewhat less, but as the flow rates increase, this pressure drop grows quicker in the sinuous microchannel as contrasted to the rectangular microchannel. Furthermore, the zigzag microchannel was shown to have a higher heat transfer efficiency than the rectangular microchannel.

In a minichannel source of heat, Ijam and Saidur [18] employed nanofluids of SiC–water and TiO_2–water in turbulent flow as coolants, and they found that they were effective. The authors were able to get a 7.25%–12.43% improvement by utilizing SiC–water, while they were able to reach a 7.63%–12.77% improvement by using TiO_2–water, according to their findings. According to Putra et al. [19], they explored the use of nanofluids as a working fluid on a heat pipe liquid block with thermoelectric cooling in order to improve overall efficiency and reduce costs. Results showed that the heat pipe liquid-block and thermoelectric cooled system using nanofluids had superior thermal performance compared to the control system. Ho et al. [20] investigated the forced convective cooling performance of a copper MCHS using an Al_2O_3/water nanofluid as a coolant in order to determine its efficiency. When tested at high pumping power, the nanofluids-cooled heat sink outperformed the

water-cooled heat sink, with a much greater average heat transfer coefficient and, as a result, significantly lower thermal resistance and wall temperature. According to the findings of Kalteh et al. [21], the Nusselt number rises with increasing Reynolds number, increasing volume concentration, and decreasing nanoparticle size inside a broad MCHS with a constant Reynolds number. However, despite the fact that the size of MCHS devices is lowering as a consequence of rapid technological advancement, the quantity of heat flux produced seems to be increasing. Because of advancements in nanotechnology, such as those made by Choi and Eastman [22] at the National Laboratories of the United States of America, these one-of-a-kind heat transfer fluids, referred to as nanofluids, have been discovered. As previously shown, nanofluids have two key advantages over more conventional fluids: (1) they are composed of milled particles or microparticles that have better thermo distribution than fluids, and (2) their temperature consistency is superior to that of fluids. According to Nguyen et al. [23], they carried out an experimental investigation of the behavior and heat transfer enhancement of Al_2O_3–water nanofluids within a closed system that was intended for cooling microprocessors or other electronic components, and their findings were published in the journal Nature Communications. When 6.8% nanofluids volume fraction was utilized in the experiment, the results demonstrated a 40% increase in heat transfer coefficient, confirming the hypothesis. Wen and Ding [24] addressing the convective heat transfer of water nanofluid in laminar flow of aluminum oxide in a copper tube. The findings were related to the convective heat transfer of water nanofluid in laminar flow of aluminum oxide. When aluminum nanoparticles are added to the nanofluid, the convection heat transfer is considerably boosted, and this rise is further amplified by raising the Reynolds number and density of the nanoparticles, as found by the researchers.

Nandha Kumar and Senthil Kumar [25] used water and ethylene glycol as base fluids to investigate the thermophysical properties of numerous nanoparticles, including ZnO, MgO, TiO_2, and Al_2O_3. The volume fraction fluctuates between 0.5% and 2.5% of the container's overall volume. According to a research published in Science, MgO–H_2O exhibited the greatest thermal conductivity at a concentration of 2.5%, with a 7.4% boost in thermal conductivity contrasted to other nanofluids. According to Jeong et al. [26], the viscosity and thermal conductivity of ZnO nanofluids with dissimilar volume fractions (0.05%–5%) were examined experimentally. Zinc oxide nanoparticles with varied sizes were employed in this study. The findings demonstrate that when the volume fraction is increased by 5%, the thermal conductivity increases by up to 18%. CuO nanoparticles with diameters ranging from 18.6 to 23.6 nm and Al_2O_3 nanoparticles with diameters ranging from 24.4 to 38.4 nm differ in two base fluids, water and ethylene glycol (EG) were examined by Lee et al. [27]. The researchers looked at four different nanofluids: CuO in EG, CuO in water, Al_2O_3 in normal water, and Al_2O_3 in dissolved EG. According to the researchers, the CuO/EG combination showed a 20% rise at 4 wt% when compared to other nanofluids.

The size of the nanoparticles itself has an impact on the viscosity and thermal conductivity of nanofluids. Eastman et al. [28] investigated the influence of Cu nanoparticle concentration and diameter on the thermal conductivity of nanofluids, and their findings were published in the journal Nature Communications. Thermal conductivity increased by 40% for nanoparticles with diameters of 20 nm when used at a concentration of 0.3%, but only by 20% when used at a concentration of 4% for nanoparticles with diameters of 23.9 nm. Working fluids were distilled water and ethylene glycol. Namburu et al. [29] looked at the effects of SiO_2 with diameters of 20, 50, and 100 nm at 6% concentrations. Their findings indicate that as the size of the nanoparticles reduces, so does the viscosity of the nanofluid. Alawi et al. [30] studied the influence of nanoparticle size on the thermal characteristics of nanofluids by conducting experiments and numerical simulations. They employed a variety of nanoparticles with diameters ranging from 25 to 100 nm, including ZnO, SiO_2, CuO, and Al_2O_3, among others. In the experiments, it was discovered that lowering the size of the nanoparticles caused an increase in the thermal conductivity of the nanofluids.

It has been hypothesized that hybrid nanofluids may be considered the next-generation fluid in the future by certain researchers. To investigate the mixing ratios of TiO_2 and SiO_2 nanoparticles, Hamid et al. [31] dabbled with five different TiO_2 and SiO_2 nanoparticle mixing ratios (20 : 80, 40 : 60, 50 : 50, 60 : 40, and 80 : 20), all of which were suspended at a concentration of 1.0% in an ethylene glycol solution composed of 60% water and 40% EG. According to the empirical evidence, all of the nanofluids had greater viscosities and thermal conductivities than the basic fluid (EG/W), which was the baseline. The nanofluid containing a TiO_2/SiO_2 combination displays the best thermal conductivity and the highest viscosity when compared to the other compositions studied in this study. The thermal conductivity and viscosity of the nanofluid made from a TiO_2/SiO_2 combination were the highest. Rimbault et al. [32] investigated the hydraulic and thermal fields of CuO–H_2O inside a rectangular MCHS, and their findings were published in their journal. When the volume concentrations of nanoparticles and the flow rate were increased in the experiment, it was revealed that the pressure drop of the nanofluid grew. As a result, the viscosity of the fluid decreased, while the pressure drop decreased as well, while the temperature of the fluid increased. Researchers discovered that heat transmission was somewhat improved at low concentrations of the chemical in issue, according to their findings (0.24% vs. 1.03%). It was discovered that when the concentration was raised to 4.5%, there was a significant increase in heat transfer. Nazari et al. [33] investigated the performance of the CPU when Al_2O_3 and CNT nanoparticles were used in various volume fractions as a nanoparticle in varied volume fractions. Clean water was injected with EG at concentrations ranging from 30% to 50%, with the EG serving as a base fluid in the experiment. In terms of temperature control, they discovered that plain water coupled with 30% EG was more effective at cooling than plain water on its own. With the use of Al_2O_3 nanofluid, the temperature was lowered by 20%, and with the

Table 1: The properties of SiC, TiO_2, and ZnO nanoparticles.

Nanoparticle	Purity (%)	Diameter (nm)	Density (g/cm^3)	Shape	Use of nanoparticle concentration (%)
SiC	99.9	<30	8.22	Spherical	0.25, 0.5, 1.5
TiO_2	99.9	<30	4.97	Spherical	0.25, 0.5, 1.5
ZnO	99.9	<30	6.6	Spherical	0.25, 0.5, 1.5

usage of CNT, the temperature was reduced by 22%. The heat transfer efficiency of Al_2O_3–H_2O and CNT–H_2O when used jointly is enhanced by 6% and 13% compared to when used individually.

In a research conducted by Sivakumar et al. [34], the performance of different nanofluids in serpentine-shaped MCHS was evaluated via the use of computational and experimental techniques. Copper microchannels with hydraulic diameters varying from 810 to 890 m were employed in this experiment. Because of its high viscosity and density, the CuO–EG nanofluid demonstrated the largest transfer coefficient and pressure drop of all the nanofluids tested. As a consequence of lowering the microchannel diameter, the heat transfer coefficient and pressure drop have both increased significantly. Additionally, Singh and Kumar [35] examined the fluid flow and heat transmission capabilities of an aluminum-based wavy rectangular MCHS with a rectangular cross section. For the purpose of increasing cooling performance, water was mixed with varying volumes of Al_2O_3. They discovered that by expanding the Reynolds number and nanoparticle concentration decreased the thermal resistance of the MCHS, which allowed them to enhance heat transfer. We measured a volume concentration of 3% at the highest point of pressure decrease. Using two different kinds of nanofluids, Thansekhar and Anbumeenakshi [36] investigated the way in which the aluminum MCHS employs the two different concentrations of H_2O–Al_2O_3 at 0.1% and 0.25%, respectively. They claimed that as compared to pure water, the heat transfer of Al_2O_3–H_2O exhibited a 36.63% improvement in efficiency. The nanofluid also resulted in a modest decrease in pressure when compared with pure water. Furthermore, Manay and Sahin [37] conducted an experimental investigation into the performance of varied concentrations of TiO_2–H_2O in microchannels to determine their effectiveness.

A broad variety of nanofluids have been intensively studied, as shown by the preceding literature survey. Despite this, there has only been a small amount of study into the performance of computer cooling systems including SiC, TiO_2, and ZnO nanoparticles suspended in a mixture of 25% ethylene glycol and 75% alkaline water. There has also been no investigation into the effects of chemically synthesized nanofluids in combination with alkaline water on fluid flow and heat transfer in computer cooling systems. The goal of this study is to look at the cooling performance of a personal computer system after adding nanoparticles in various concentrations in base fluid at different temperatures. When testing the cooling system under real-world settings, researchers employed a genuine computer configuration with a land grid array 775 Electric socket for the CPU to determine the impact of the cooling systems may efficiently utilizing nanofluids and conventional fluids.

2. Nanofluid Preparation and Characterization

High energy consumption, poor purity, uneven particle size distribution, large volumes of secondary waste, and long-term environmental damage are only some of the problems associated with physical processes. Chemical processes, on the other hand, benefit from low energy consumption, high purity, consistent particle size distribution, low cost, and minimum environmental impact. It is becoming more important to synthesize ZnO materials in ecologically benign methods as the number of ZnO uses grows, especially now that the public's expectations for environmental preservation have been instilled according to Anbuvannan et al. [38]. Use of microorganisms, plant extract, and plant enzymes in the chemical reaction process is a green synthesis approach. The production of ZnO may be stabilized and reduced by extracts from plants such as peels, flowers, fruits, and seeds, as well as from leaves, peels, roots, and other parts of the plant. ZnO formation may be reduced and stabilized by using these extracts, according to research. It is possible to make zinc oxide using plant extracts, which results in a zinc oxide that is more effective against a wide spectrum of bacteria than chemically synthesized zinc oxide was investigated by Vijayakumar et al. [39]. To use these compounds in products that will come into contact with the human body, they must be nontoxic and mild. Environmentally friendly growth may be facilitated by the use of plant extracts in the production of green zinc oxide in the future. This approach is used to manufacture nanoparticles from extracts of the Hibiscus Rosa-Sinensis leaf, which is the subject of this research. A leaf extract of roughly 50 mL was obtained and heated at 70°C with a stirrer for 15 min. Due to the high temperature, 5 g of zinc nitrate was added to the solution before it was applied. Cooking happens before the addition of a yellow-colored paste to the mixture. A ceramic crucible was used to collect the paste, which was heated in a furnace at 400°C for 2 h to collect the paste. It produces a powder of a soft white tint that may be collected and utilized for a variety of other uses. Nanofluids are created using chemically generated SiC, TiO_2, and ZnO nanoparticles with diameters ranging from 20 nm to 99% purity, which has been purified to 99% purity. CTAB, a surfactant, is also used to prepare these particles, and it is used to do so. The following is the procedure to be followed to create nanofluids: the solution should be added to dilute water and then treated to an ultrasonic granulator for 30 min to get the optimum results. To get the desired amplitude, the ultrasonic-aided machining vibrator is set to 0.6 on the scale. It is used in the vibration of SiC, TiO_2, and ZnO nanoparticles. In Table 1, you can see the nanoparticle properties. Images of spherical-shaped SiC, TiO_2, and ZnO nanoparticles were acquired using scanning electron microscopy

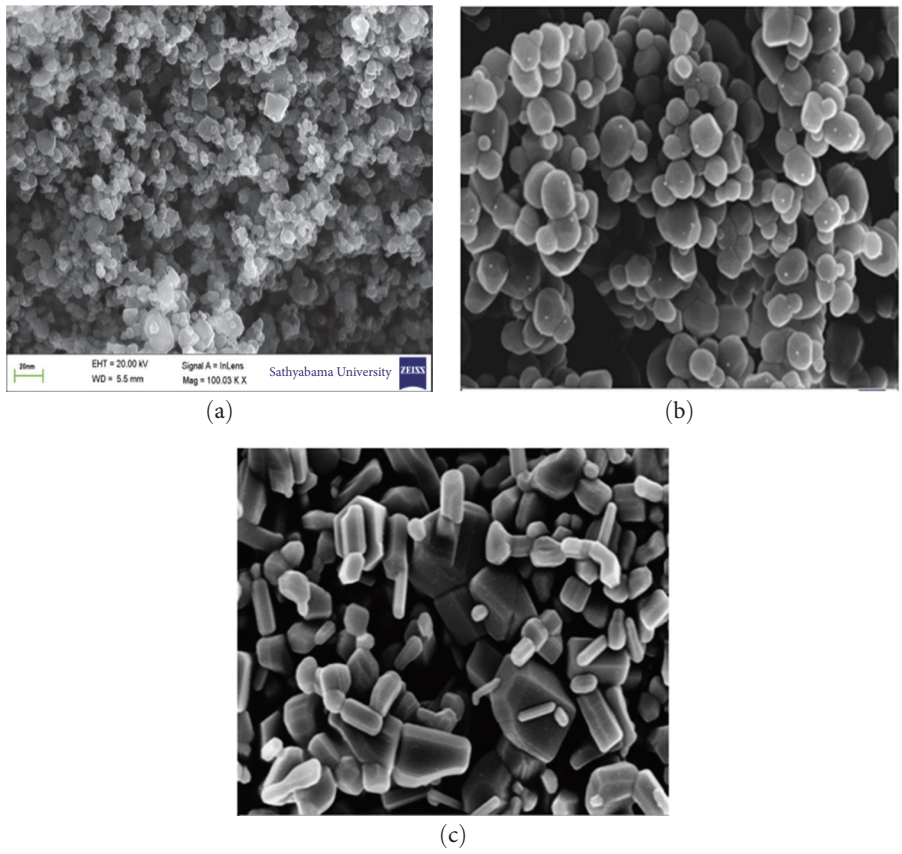

Figure 1: SEM (a) SiC, (b) TiO_2, and (c) ZnO.

(SEM) as shown in Figure 1. The images were acquired using SEM and XRD after the nanoparticles were received from the manufacturer. To ensure that all of the nanoparticles were pure and had diameters less than 50 nm, SEM and XRD were utilized. A goniometer is an angle measurement equipment that is particularly helpful for measuring the angles between the faces of crystals. Goniometer uses CuK-alpha radiation in the two-range of 10–80 nm for the X-ray diffractometer, which is a wavelength between 10 and 80 nm. The Debye–Scherrer formula is used in XRD analysis to compute the starting condition and measurement in a goniometer with a radius of 217.5 mm, a step duration of (30.6) s, and a step size of 30.6 nm (0.0289093). The greatest intensity detected in this analysis is 67.45° out of 1,125 counts, which is the highest attainable. Peak intensity levels and wide diffraction patterns show crystallinity, which suggests that the particles under study have an extremely tiny crystallite size which is shown in Figure 1.

During an hour-long experiment, an ultrasonic probe blender was deployed to disperse the nanoparticles in solution and reduce agglomeration. Using an ultrasonic probe, pulses with utmost power of 500 W and a frequency of 20 kHz may be generated by the device. The presence of surfactants may have an effect on the thermal characteristics of nanofluids, which is why none were used in this experiment. It was decided to adopt the observation approach for this experiment since it has already been proved to be advantageous. Nanofluids containing silicon carbide, titanium oxide, and zinc oxide were stable for 2 weeks at concentrations of 0.25%, 0.5%, and 1.5% for the same period of time.

3. Thermophysical Properties

It is possible to determine the thermal conductivity of nanofluids by using the transient hot-wire approach, which is an operating mechanism that has been developed. A KD2 Pro thermal analyzer was used to test the thermal conductivity of the SiC–EG/AW, TiO_2–EG/AW, and ZnO–EG/AW nanofluids to a precision of $\mp 5\%$. Thermal conductivity tests were taken at 25°C. At the same temperature as the previous experiments, the viscosities of nanofluids with concentrations ranging from 0.25% to 1.5% were determined using a Bonvoisin digital rotary viscometer. According to this notion, the base fluid EG/AW (25 : 75) is also assumed to have a significant role in defining the density of the nanofluid through influencing the density of the nanofluid. As previously stated, the size and shape of the nanoparticles were not taken into consideration since they have no effect on the density of the particles. The density of the nanofluids was determined with the use of a pycnometer. Data verification was carried out using the base fluid EG/AW (25 : 75), which was used to initiate the measurements (thermal conductivity, density, and viscosity). For the purposes of analysis, all measures were taken three times and the averages of these values were utilized to make the

Table 2: Thermal and physical attributes of nanofluids at 25°C.

Working fluid	Concentration	K(W/m·K)	c_p(J/kg·K)	ρ(kg/m^2)	μ(Ns/m^2)
Base fluid	0	0.578	3,928	1,529	0.00187
SiC–EG/AW	0.25	0.627	3,813	1,257	0.00199
	0.5	0.645	3,505	1,289	0.88183
	1.5	0.657	3,306	1,292	0.00178
TiO_2–EG/AW	0.25	0.645	3,871	1,220	0.00173
	0.5	0.652	3,827	1,238	0.00176
	1.5	0.675	3,732	1,276	0.00188
ZnO–EG/AW	0.25	0.623	3,737	1,237	0.00168
	0.5	0.679	3,827	1,256	0.00181
	1.5	0.675	3,732	1,269	0.00197

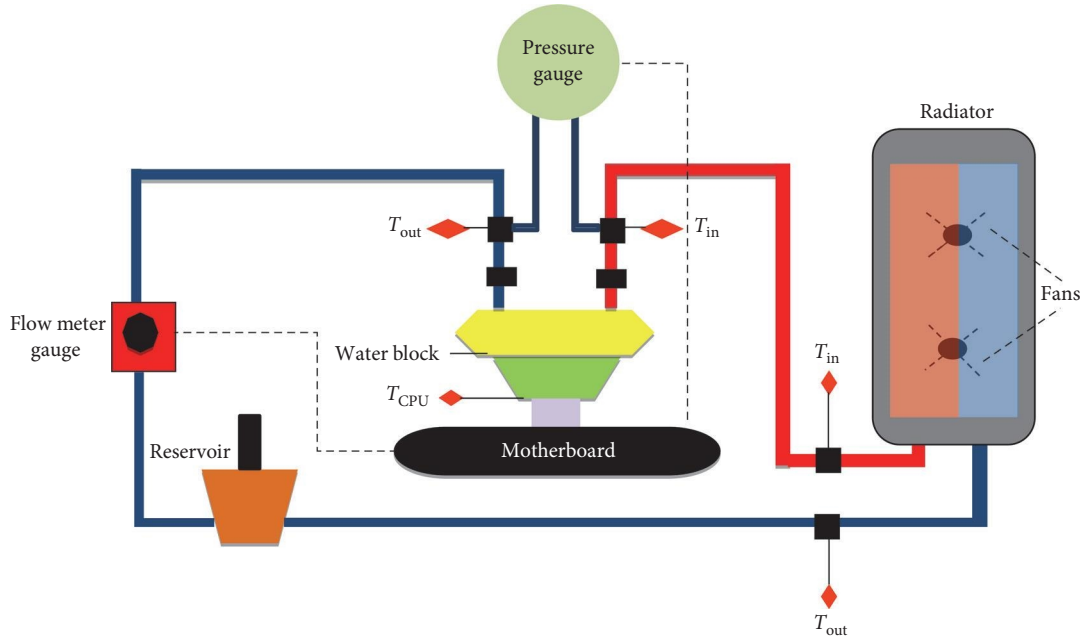

Figure 2: A schematic illustration of the test design.

final decision. The specific heat, on the other hand, may be simply calculated using Equation (1) [40].

$$C_{nf} = \frac{(1-\varphi)(\rho C)_{bf} + \varphi(\rho C)_{np}}{\rho_{nf}}. \quad (1)$$

To demonstrate this, Table 2 illustrates the thermophysical characteristics of silicon carbide, titanium oxide, and zinc oxide nanoparticles suspended in EG/AW (25 : 75) solutions of 0.25%, one-tenth of 0.5%, and two-tenths of 1.5% concentrations at 25°C.

4. Experimental Setup

The thermal and heat transfer performance of the computer cooling system on the CPU was investigated in an experimental environment using nanofluids and base fluid. Figure 2 depicts a schematic representation of the whole experimental setup, which includes all of the components. A computer cooling system (water block, radiator, fans, pump, reservoir, tubes, and fitting), a motherboard (CPU, power supply, and external hard drive), and sensors (such as temperature and humidity sensors) are all part of the system (pressure sensor, temperature sensors, flow meter sensor). In this experiment, the EKWB EK-KIT S240 computer cooling system was utilized to cool the PC. Water block, radiator, fans, a pump, a storage tank, tubing, and fittings are all part of the package. The water block has the following dimensions: $(54 \times 54 \times 20)$ mm^3 and is made up of two parts: a base and a top. The acrylic top and copper bottom sides of this sculpture are inextricably bound together. The fluid in and out ports of the water block are permanently attached to the top of the cover, making it easy to access and repair. With 50 channels with a width of 0.2 mm, a height of 2 mm, and a length of 32 mm, the copper foundation (MCHS) of the water block provides excellent thermal conductivity.

The integrated reservoir pump (D5 pump) has a maximum flow rate of 1,500 L/hr, which is the maximum flow

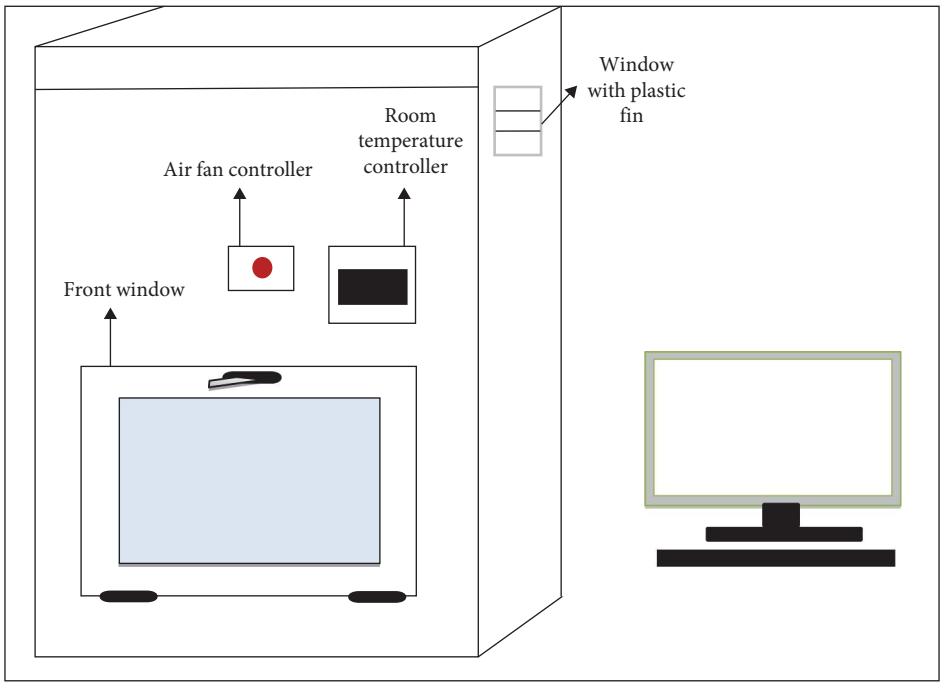

Figure 3: Microchannel heat sink with water block in an insulated room.

rate available. Because it incorporates a unique rubber shock absorber, it is quieter and generates less noise while in operation than a standard vacuum cleaner. Two fans spinning at 1,200 rpm were installed on the radiator. Heat transmission is enhanced by the use of copper fins and tubes, which provide a large surface area for heat transfer. A variety of tubes and fittings were used to connect the various components of the experiment together.

Because it has the greatest hardware engineering, the most innovative concepts, and the quickest performance, an ASUS X48 motherboard was utilized in the experiment. Additionally, while the CPU is operating, the frequency and voltage of the processor may be raised, resulting in the generation of extra heat. Because of the increased overclocking capability, the frequency and voltage may be increased, resulting in increased heat output. The connection between the CPU and the motherboard is made by a surface-mount connector known as an lang grid array (LGA) surface-mount socket. Socket LGA775 is often referred to as such due to the fact that it has 775 connections arranged in two cores on its surface. The thermal interface (8.5 W/(mK)) was applied to the top surface of the CPU to guarantee that the temperature was distributed evenly throughout the surface since it is a good heat transfer medium. Also installed above the CPU interface was a flat temperature sensor for recording the temperature of the water block's base heat sinks, which was fixed above the CPU interface, shown in Figure 3.

The coolant is pushed to the water block by the pump at a variety of mass flow rates, including 0.025, 0.052, and 0.080 kg/s, respectively. Speed of the pump is regulated by a specific controller that was developed in the laboratories. Aqua software was used to record the mass flow of the working fluid. The intake and exit ports of the water block are equipped with LCD temperature sensors and a pressure drop sensor in order to gather data on convective heat transfer characteristics. There is a wide range of temperatures that LCD temperature sensors can measure, from 40 to 70°C. Throughout the experiment, all of the temperature readings have been recorded on a digital screen using a digital camera. In order to remove the heat, the coolant is pushed from the water block to a massive radiator, where it is recirculated many times. All of the tubes were wrapped with rubber foam insulation to prevent any heat transmission to the surrounding environment during the manufacturing process. The experimental investigation was performed several times on various days in order to confirm that the experiment was repeatable. Following the studies, it was discovered that just a small number of nanoparticles were adhering to the surface of the MCHS. Nevertheless, after taking the tests, the MCHS surface seemed to be clean and free of corrosion.

5. Data Processing

An important parameter to consider is the coefficient of heat transfer between the base fluid and the water slab block. Researchers have analyzed it in line with Newton's cooling rule [41].

$$q = h \cdot \mathrm{A} \Delta T_{\mathrm{m}}, \tag{2}$$

where q is the rate at which heat is created in the CPU, h signifies the heat transfer coefficient, and T_{m} is the working fluid and the MCHS walls are separated by a log mean temperature difference, as specified in greater detail below [42].

A is the area of heat transfer, and ΔT_m is the area of heat transfer.

$$\Delta T_m = \frac{T_{out} - T_{in}}{\ln \dfrac{T_{hsbt} - T_{in}}{T_{hsbt} - T_{out}}}. \tag{3}$$

The fluid temperatures at the water block's intake and outflow are T_{out} and T_{in}, respectively, while the heat sink's base temperature, T_{hsbt}, is taken as constant throughout. When the base fluid is passed through the water slab block, the temperature rises as a result of the heat absorbed by the water block [43].

$$q = \dot{m} \cdot C_{bf,nf}(T_{out} - T_{in}). \tag{4}$$

For example, if the mass flow rate is $\dot{m}$ (in kilograms per second), the specific heat of the conventional fluids is $C_{bf,nf}$ (kg·K).

The convective heat transfer coefficient may be expressed as [44] by equating Equations (2) and (4).

$$h = \frac{\dot{m} \cdot C_{bf,nf}(T_{out} - T_{in})}{A \dfrac{T_{out-T_{in}}}{\ln \dfrac{T_{hsbt} - T_{in}}{T_{hsbt} - T_{out}}}}. \tag{5}$$

The following equation has been used to compute the pumping power.

$$P_p = \frac{\dot{m}}{\rho_{bf,nf}} \Delta P, \tag{6}$$

where $\dot{m}$ is the mass flow rate, $\rho_{bf,nf}$ is the density of the base fluid and nanofluid, ΔP is the absolute value of the pressure drop.

6. Thermophysical Properties of Nanofluids

It is necessary to determine the thermal conductivity of nanofluid from the outset to establish an agreeable agreement between theoretical and experimental data. The H–C model [45] is used to estimate the thermophysical characteristics of nanofluids. In most fluid thermal conductivity calculations, this model is used.

$$k_{nf} = \left[\frac{k_p + (m-1)k_t - (m-1)\varphi(k_t - k_p)}{k_p + (m-1)k_t + \varphi(k_t - k_p)}\right] k_t. \tag{7}$$

These are two characteristics of spherical particles that may be assessed based on their thermal conductivity: the empirical form factor N and the sphericity. It is one when considering the sphericality of a spherical item. The thermal conductivity of nanoparticles and the thermal conductivity of base fluids are denoted by the letters k_{nf} and k_p, respectively. Murshed et al. [46] estimated the thermal conductivity of nanofluids, Bruggeman developed the following model, which can be expressed mathematically as:

$$k_{nf} = 0.25\left[(3\varphi - 1)k_p + (2 - 3\varphi)k_t\right] + \frac{k_t}{4}\sqrt{\Delta}. \tag{8}$$

$$\Delta = \left[(3\varphi - 1)^2 (k_p/k_t)^2 + (2 - 3\varphi)^2 + 2(2 + 9\varphi - 9\varphi^2)(k_p k_t)\right]. \tag{9}$$

Yu and Choi [47] suggested the following new mathematical equation for estimating thermal conductivity:

$$k_{nf} = \left[\frac{k_p + 2k_t - 2\varphi(k_t - k_p)(1+\beta)^3\varphi}{k_p + 2k_t + \varphi(k_t - k_p)(1+\beta)^3\varphi}\right] k_t, \tag{10}$$

where β is the ratio of nanolayer thickness to original particle radius. The thermal efficiency of a nanofluid is calculated using $b = 0.1$. The notion of the effective medium, introduced by Timofeeva et al. [48], is used to compute thermal conductivity of nanofluids and is stated as follows:

$$k_{nf} = [1 + 3\varphi]k_t. \tag{11}$$

It is possible to determine the thermal conductivity of microfluids by using many theoretical methodologies. The viscosity of a nanofluid is a significant component in influencing its performance. This research examines how well-known models predict outcomes and compares them to the actual findings. Batchelor [49] recommends that viscosity be calculated using a straightforward equation for fluids containing sphere-shaped nanoparticles.

$$\mu_{nf} = (1 + 2.5\varphi + 6.2\varphi^2)\mu_t. \tag{12}$$

The Einstein equation for determining the viscosity of spherical particles of volume is proposed by Drew and Passman [50].

$$\mu_{nf} = (1 + 2.5\varphi)\mu_t. \tag{13}$$

Brinkman [51] reduced Einstein's equation to a simple mathematical structure, which is represented as follows:

$$\mu_{nf} = \frac{1}{(1-\varphi)^{2.5}}\mu_t. \tag{14}$$

Wang et al. [52] proposed a model for calculating nanofluid viscosity, which can be stated as:

$$\mu_{nf} = (1 + 7.3\varphi + 123\varphi^2)\mu_t, \tag{15}$$

where φ is the molecule volumetric fixation, μ_{nf} is the consistency of the nanofluid and μ_t is the thickness of the therminol or the base liquid.

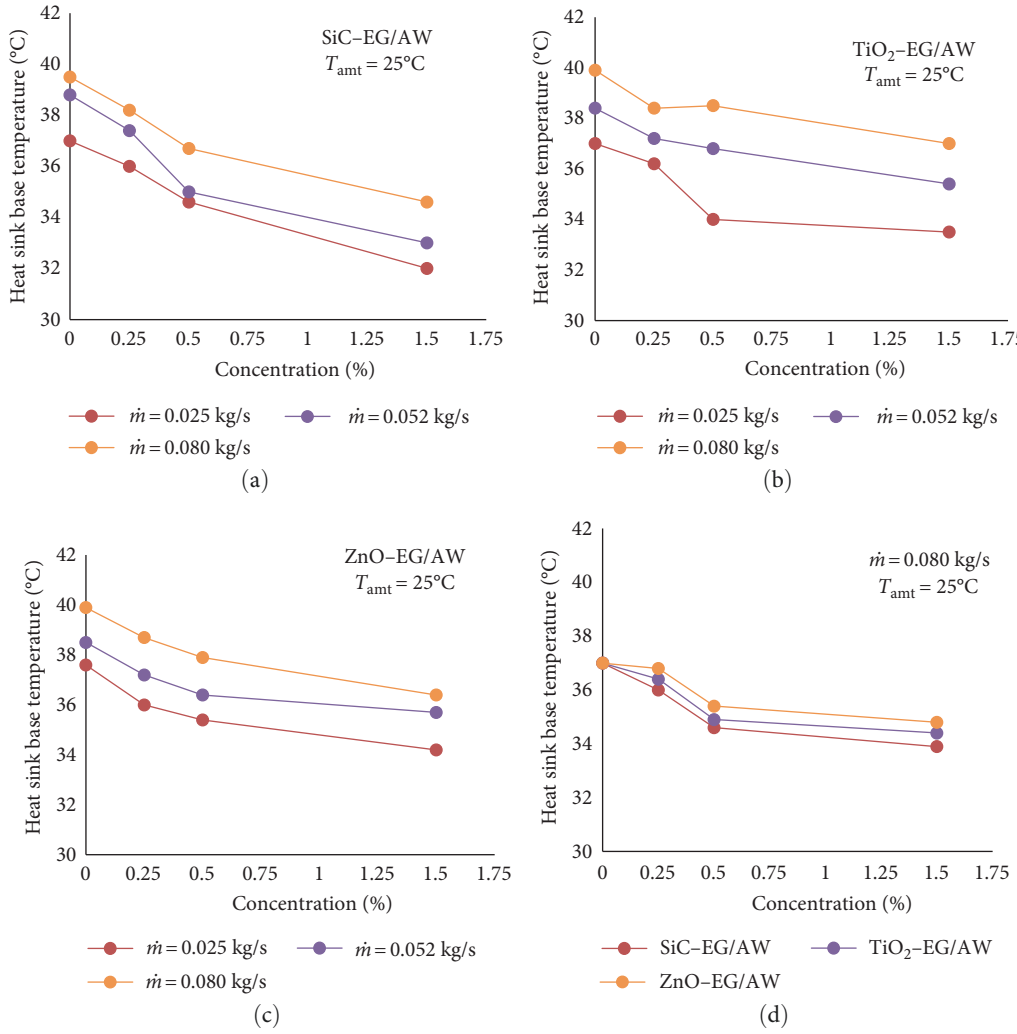

Figure 4: Nanofluid concentrations in relation to the heat sink's temperature at different mass flow rates: (a) SiC–EG/AW; (b) TiO_2–EG/AW; (c) ZnO–EG/AW; (d) a variety of nanofluids.

7. Discussion on Findings

The primary goal of the computer cooling system is to ensure the lowest feasible operating temperatures for the heat sink and CPU. As the CPU load rose, the temperature of the heat sink's base was monitored to ensure that it did not overheat and cause damage. The base temperature of the heat sink was monitored between the heated source and the water block, and the results were utilized to determine the total efficiency of the cooling system. A flat temperature sensor was put between the base of the heat sink and the CPU's core temperature measurement point. Figure 4(a)–4(c) depicts the relationship between heat sink base temperature and nanoparticle concentration, which ranges from 0.25% to 1.5% in the heat sink, as represented by the SiC–EG/AW, TiO_2–EG/AW, and ZnO–EG/AW nanoparticles in the heat sink. Three distinct mass flow rates of nanofluids and base fluid were used in the experiment: 0.025, 0.052, and 0.089 kg/s. The results of the experiment were compared. To analyze the nanofluids and base fluid, three different mass flow rates were employed in the experiment. The temperature in the room was kept constant at 25°C. The base temperatures of heat sinks were also shown as a function of base fluid concentration at various mass flow rates, with 0% concentration showing that there was no base fluid concentration at any point.

According to Figure 4(a)–4(b), when the computer cooling fluid is infused with nanoparticles, together with an increase in the volumetric flow rate, resulted in more heat evacuation from the heated slab block and maintained the interlinking temperature to a minimum. This was shown to be true for all three nanoparticles that were employed in this study. As shown in Figure 4(a), the effects of various concentrations of SiC–EG/AW on the heat sink base temperature were investigated. The concentrations used were 0%, 0.25%, 0.5%, and 1.5%. It can be plainly observed that raising the mass flow rate to 0.080 kg/s and the concentration of the nanoparticles to 1.5% may result in a reduction in the heat sink base temperature from 37.5 to 34.7°C. As demonstrated in Figures 4(b) and 4(c), using TiO_2–EG/AW as a working fluid with the same mass flow rate and concentration may

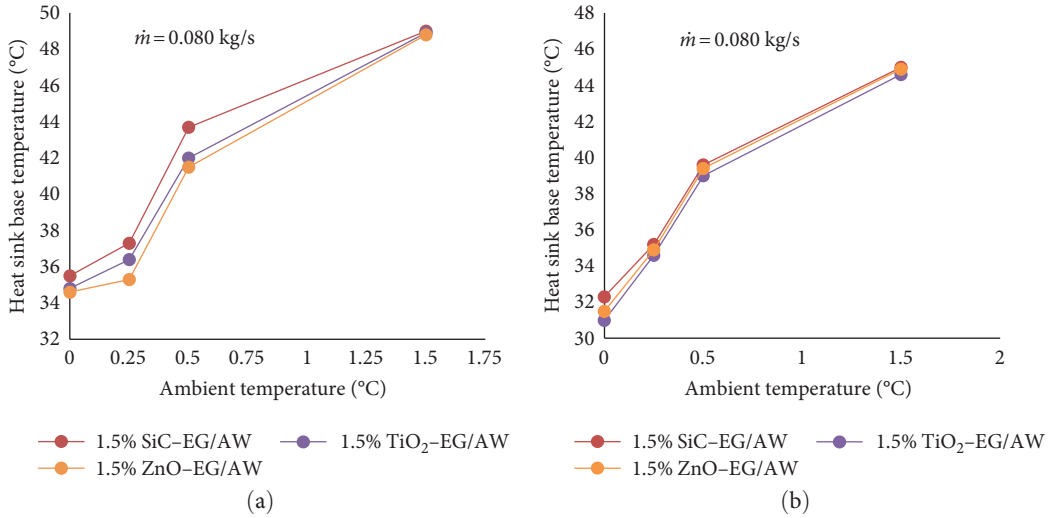

FIGURE 5: (a) The base temperature of a heat sink; (b) the fluid temperature of several nanofluids is compared to the ambient temperature.

reduce the temperature of the heat sink from 37.5 to 35.4°C and from 37.5 to 35.8°C, respectively. As shown in Figure 4(d), using ZnO–EG/AW at a 1.5% concentration as a working fluid in a computer cooling system reduced the base temperature of the heat sink by 8.9% compared to using the base fluid. At 25°C, ZnO–EG/AW at 1.5% reduced temperature by 7.1%, whereas TiO_2–EG/AW reduced temperature by 4.9%. Both results are compared to 0% base fluid. As a result of the high viscosity of the SiC–EG/AW at a 1.5% concentration, a hydraulic thickening occurs, which results in a thickening of the thermal boundary layer.

As a consequence, when contrasted to the other nanofluids explored, SiC–EG/AW has the lowest heat sink temperature because it has the maximum stiffness and thermal expansion. As a result, it has the lowest heat sink temperature when compared to the other nanofluids researched. The results in Figure 5 demonstrate that the effect of ambient temperature on the heat sink base temperature and fluid temperature varied from 25 to 40°C when using nanofluids such as SiC–EG/AW and TiO_2–EG/AW at a concentration of 1.5% and a flow rate of 0.080 kg/s. Heat sink base and base fluid temperatures, as well as nanofluid temperatures, are expected to rise as a consequence of increased ambient temperatures, as seen in these figures. The heat flux increases as a consequence of the increased temperature of the processor as a result of the increased temperature of the surrounding environment.

The fact that many experts believe that raising the rate of flow by increasing the pump speed might result in undesirable noise should be highlighted, as previously stated. However, in this study, a D5 (pulse-width modulation) pump was utilized, which functions quietly even while operating at high speeds due to the usage of a specific rubber cushion absorber.

8. Heat Transfer Coefficients

The primary goal of this study is to assess the thermal performance of nanofluids and how it ramifications the cooling system as well as the computing power of computers. It has been revealed that the convective heat transfer coefficient of nanofluids has an influence on their thermal performance, according to a number of surveys. On the other hand, Figure 6(a)–6(d) illustrates the relationship between the heat transfer coefficient and the concentrations of SiC–EG/AW, TiO_2–EG/AW, and ZnO–EG/AW nanoparticles, respectively (0.25%, 0.5%, and 1.5%, respectively). While operating at 25°C in the ambient environment, the mass flow rates for the base fluid and nanofluids are each 0.025 kg/s for the base fluid and 0.052 kg/s for the nanofluids, respectively. It is assumed that the concentration of EG/AW in the base fluid is 0% in proportion to the base fluid EG/AW (25 : 75). It can be observed in the figures that raising the mass flow rates while simultaneously introducing nanoparticles into the base fluid results in an increase in the heat transfer coefficient of the base fluid. Increased Brownian motion and thermal conductivity of the working fluid are anticipated to result in improved thermal performance of the nanofluid over the foundation fluid.

In contrast, raising the mass flow rate to 0.080 kg/s while simultaneously increasing the concentration to 1.5% resulted in the maximum feasible heat transfer coefficient, according to the calculations. When the mass flow rate is increased from 0.084 to 0.084 kg/s, the heat transfer coefficient of SiC–EG/AW increases from 7,931 to 11,112 $W/(m^2 K)$. When the concentration of the nanoparticles is increased from 0% to 1.5%, the heat transfer coefficient of SiC–EG/AW increases from 7,931 to 11,112 $W/(m^2 K)$. In addition, when SiC–EG/AW and TiO_2–EG/AW are used as working fluids, the heat transfer rate rises from 8,031 to 11,619 $W/(m^2 K)$ and from 8,031 to 9,924 $W/(m^2 K)$, respectively, however when the other working fluids are employed, the heat transfer rate remains constant (see Figure 6(b)–6(c)). The highest heat transfer coefficient is achieved by using SiC–EG/AW at a concentration of 1.5% and an ambient temperature of 25°C, resulting in a 31% improvement over the base fluid.

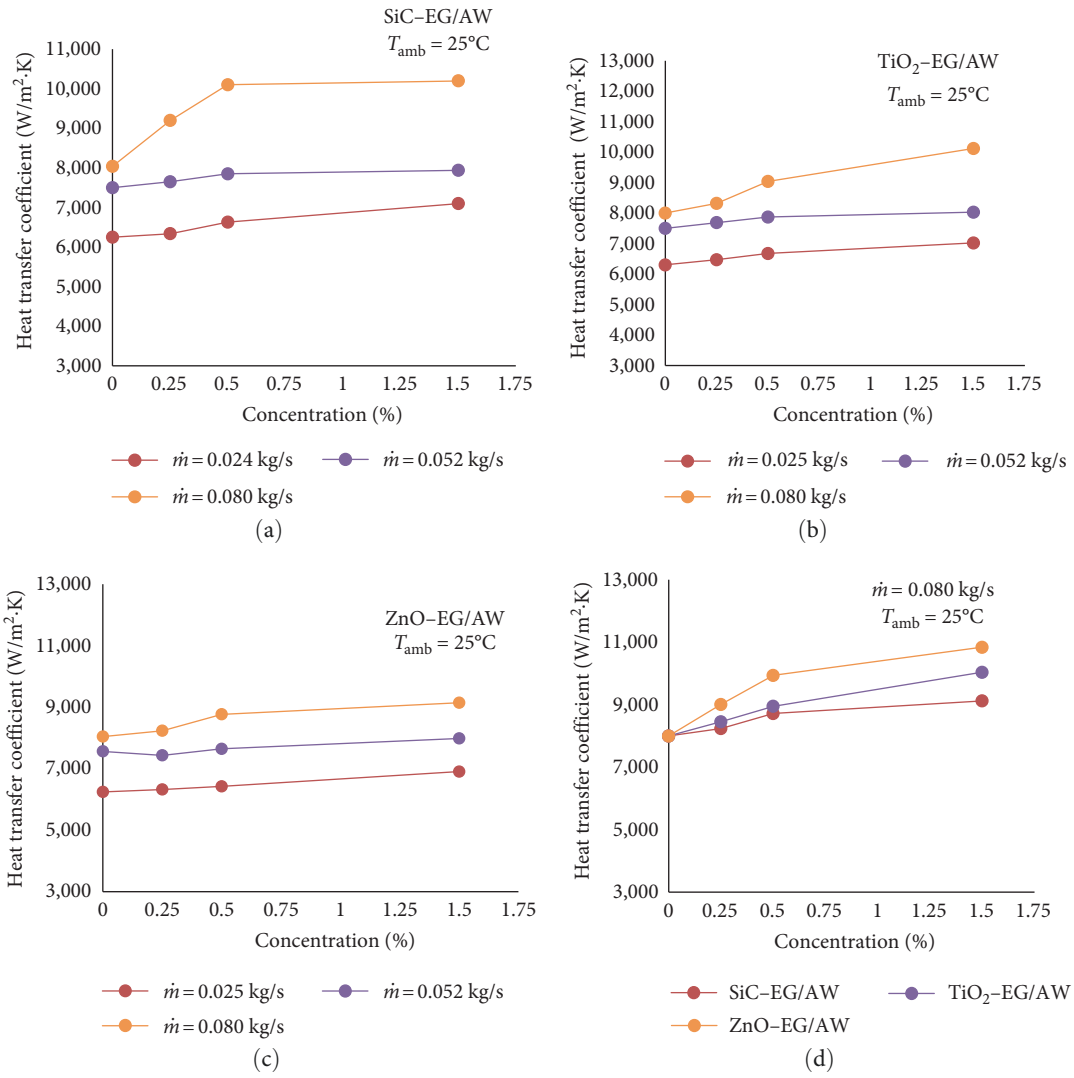

Figure 6: Heat transfer coefficient vs. nanoparticle concentration in nanofluids: (a) SiC–EG/AW; (b) TiO_2–EG/AW; (c) ZnO–EG/AW; (d) disparate nanofluids.

This is followed by TiO_2–EG/AW at a concentration of 24% and ZnO–EG/AW at a concentration of 19%, both with improvements of 24% and 19% relative to the base fluid, respectively. The high heat conductivity and viscosity of the SiC–EG/AW, which both contribute to the observed behavior, make it difficult to determine the cause of the observed behavior.

Even at low flow rates, the fact that Pr and rise more than Re drops as a result of the increase in viscosity can be seen, showing that the heat transfer coefficient rises as the concentration of the solution increases. As a result of the rise in viscosity, Pr and increase more than Re decreases. Because of this, as can be seen in the graph below, the convection heat transfer coefficient rises as a function of thermal conductivity, Prandtl number, and Reynolds number (h, Pr, Re). In addition, when the flow rate is increased, a significant rise in the heat transfer coefficient is seen as a result. Using SiC–EG/AW nanofluids at a 1.5% concentration and a mass flow rate of 0.080 kg/s, Figure 7 depicts the impact of temperature

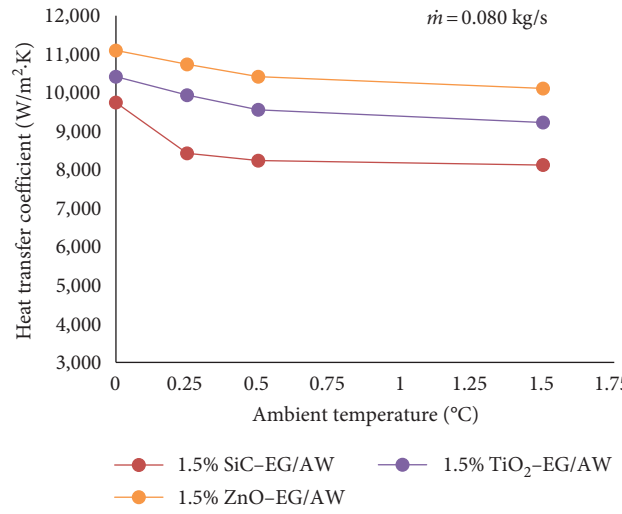

Figure 7: Temperature-dependent heat transfer coefficients exist for several nanofluids.

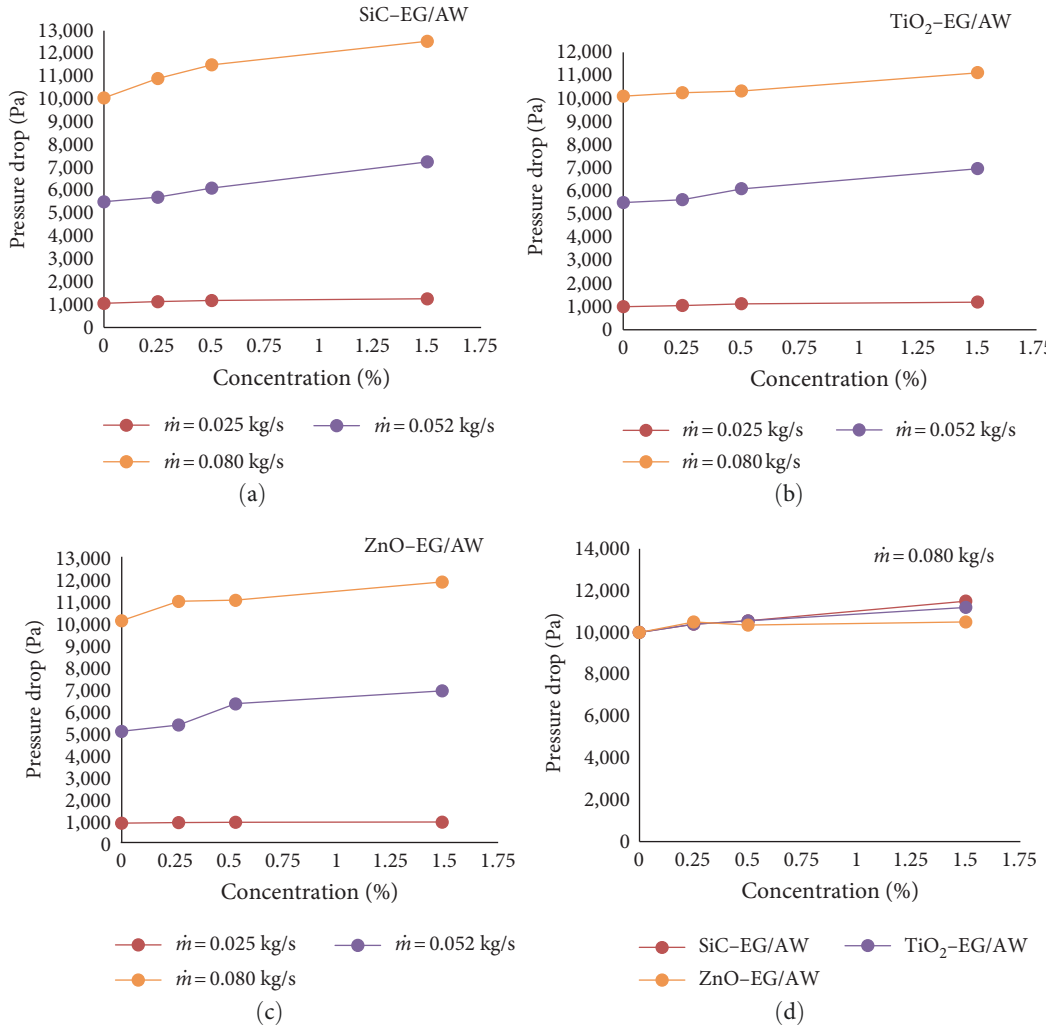

Figure 8: Pressure reduction vs. nanoparticle concentrations using nanofluids: (a) SiC–EG/AW; (b) TiO_2–EG/AW; (c) ZnO–EG/AW; (d) nanofluids of various types.

change on the heat transfer coefficient when the ambient temperature is changed. According to what can be seen, increasing the heat from the surrounding environment causes a reduction in the heat transfer coefficient of all nanofluids, which can be seen. Heat flow increases as a result of an increase in the temperature difference between the cooling fluid and heat sink base temperature. As a result of these linked effects, the heat transfer coefficient for a constant heat transfer surface decreases for any given constant heating surface.

9. Pressure Drop

Observing the pressure decrease in the base fluid after the nanoparticles have been introduced into the base fluid is essential for determining whether or not the use of nanoparticles is advantageous to the cooling process. As the working fluid goes through the water block and into the microchannels, the pressure of the working fluid decreases. Modeling the pressure drop of a base fluid and nanofluids ((a) SiC–EG/AW, (b) TiO_2–EG/AW, and (c) ZnO–EG/AW) at concentrations ranging from 0% to 1.5% and mass flow rates of 0.025 to 0.080 kg/s, respectively, is shown in Figure 8(a)–8(d). Overall, all of the photographs demonstrate that when the mass flow and nanoparticle concentration of the nanofluids increase, the pressure in the water block falls, as seen in Figure 1. The evidence given in the results lends weight to this assertion. As a consequence of the inclusion of nanoparticles in the formulation, the density and kinematic viscosity of the base fluid both increases, resulting in an increase in the pressure drop; as the mass flow rate, and therefore, the fluid velocity (w) increases, the pressure decrease increases even more.

A modest rise in the drop in pressure may be noticed, as shown in Figure 8(d), when the concentration of all nanofluids is raised from 0% to 1.5% as shown in Figure 8(a). The smallest pressure drop is attained by SiC–EG/AW, which is followed by TiO_2–EG/AW and SiC–EG/AW, both of which are in the top three. This is due to the fact that TiO_2–EG/AW has a Contrary to the other nanofluids, it seems to have a

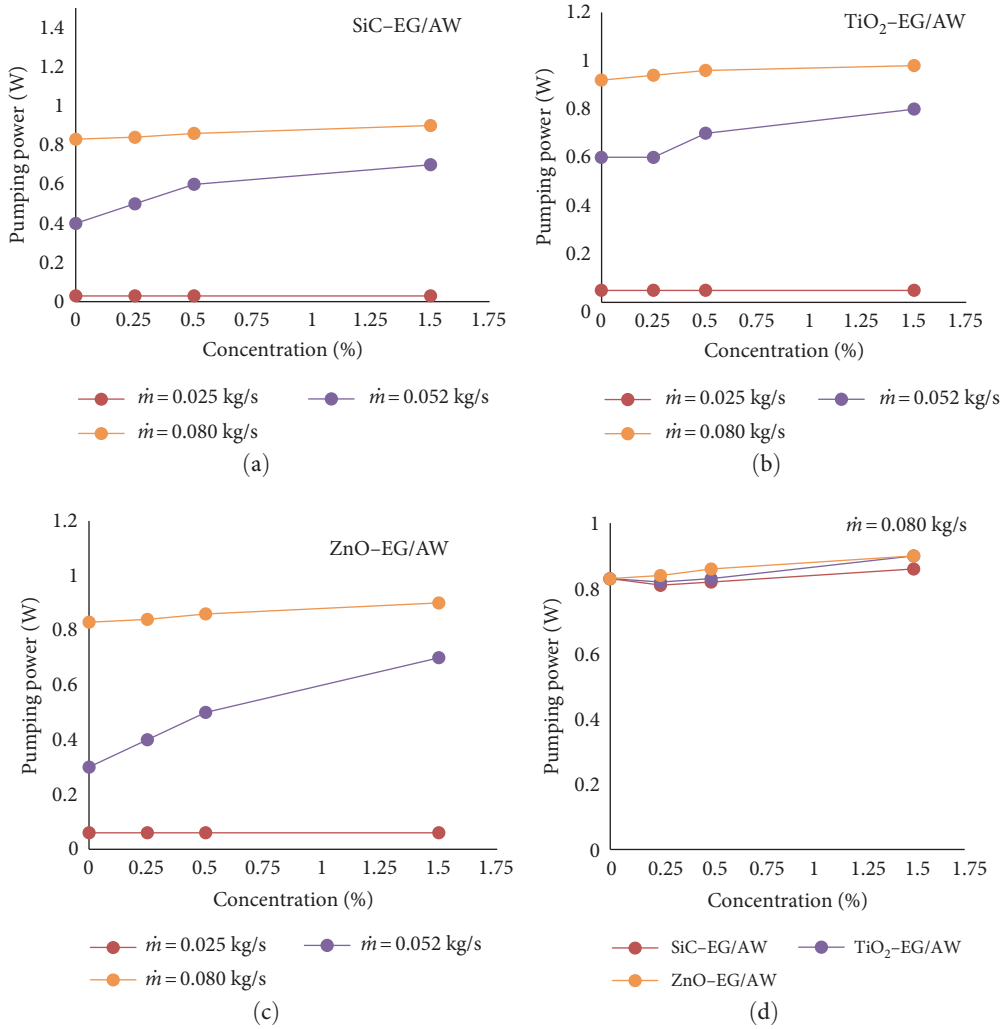

FIGURE 9: Pumping power vs. concentration of nanoparticles in nanofluids at distinct flow rate: (a) SiC–EG/AW; (b) TiO_2–EG/AW; (c) ZnO–EG/AW; (d) nanofluids of various types.

lower viscosity. When used at a concentration of 0.5%, the SiC and ZnO nanofluids provide results that are almost identical; however, when the concentration is raised to 1.5%, the difference becomes more obvious.

10. Pumping Power

Nanofluids should increase the heat transfer qualities of computer applications while without considerably increasing the pumping power necessary to run them as a fluid that is reliable in dissipating heat. Whenever the working fluid is pumped through the small heat sink channels in the system, the pressure in the system decreases somewhat and viscosity increases. In order to compensate for the pressure loss, the system needs extra pumping power. Figure 9(a)–9(d) depicts the relationship between pumping power and nanoparticle concentrations in a nanofluid at various mass fluxes, including 0.025, 0.052, and 0.080 kg/s, respectively. The addition of nanoparticles to the base fluid has been demonstrated to result in a modest increase in pumping power, which is more than compensated by the nanofluid's improved thermal performance. Despite this, TiO_2–EG/AWhas the lowest pumping power, whereas SiC–EG/AW and ZnO–EG/AW have performance values that are fairly similar. According to Equation (6), the pumping power follows the pressure reduction trend, which is amplified by the fluid velocity measurement.

11. Conclusions

Researchers conducted a pilot study to determine the influence of employing several kinds of nanofluids in cooling of computer systems on the performance of the systems. In this work, three different types of nanoparticles were used: SiC, TiO_2, and ZnO nanoparticles, which were suspended in a solution of 25% ethylene glycol and 75% alkaline water. Both the experimental setting and the methodologies used in the experiment were thoroughly explored. All of the following variables have been explored experimentally: CPU temperature, air temperature, heat transfer rate of the working fluids and nanofluids in MCHS, pressure slant of the

working fluids and nanofluids in MCHS, and MCHS pumping power.

The results demonstrate that:

(1) Elevated nanoparticle concentration from 0.25% to 1.5% while concurrently increasing mass flow resulted in a reduction in base temperature that is larger than the reduction in base fluid temperature in a heat sink. Because SiC nanofluid exhibited the highest thermal conductivity and viscosity of all of the nanofluids tested, using a 1.5% concentration of SiC nanofluid resulted in an 8.9% drop in temperature. Temperature drops by 6.9% and 4.9% respectively, when compared to the base fluid EG/AW, when the TiO_2 and ZnO nanofluids have the same concentration of TiO_2 and ZnO, when compared to the base fluid EG/AW, when compared to the base fluid EG/AW (25 : 75). When the temperature of the surrounding environment was elevated from 25 to 40°C, the basal temperature of the heat sink climbed

(2) A significant increase in the heat transfer rate is seen when nanoparticles are added to a base fluid in conjunction with an increase in the mass flow rate as compared to the base fluid alone. With a 31% increase in heat transfer coefficient, the SiC nanofluid demonstrates the biggest increase in heat transfer coefficient, while the TiO_2 nanofluid exhibits a 26% increase in heat transfer coefficient. The ZnO showed a 19% boost in performance over the control. Increased ambient temperature from 25 to 40°C resulted in a drop in the heat transfer coefficient as a secondary effect

(3) Flow and concentration of nanofluid both increases, resulting in reduced pressure and perhaps more pumping power. The lowest number is TiO_2–EG/AW, which is followed by ZnO–EG/AW and SiC–EG/AW, both of which are in the top three. However, the nanofluid's considerable improvement in computer cooling performance over the basic fluid may compensate for the modest increase in pumping power and pressure loss

(4) When it comes to computer cooling systems, this work is groundbreaking since it provides previously accessible information on the comparative behavior of SiC, TiO_2, and ZnO nanoparticles detach in EG/AW (25 : 75) when utilized as cooling fluids. A set of graphs is shown that depicts the fluctuation in the convective heat transfer coefficient, heat sink base temperature, pressure decline, and pumping power as a function of the nanoparticle attentiveness in nanofluids and the rate of mass flow of the cooling fluid, respectively

Data Availability

The authors affirm that the data supporting the conclusions of this research can be found inside the article, which they believe is correct.

Conflicts of Interest

The authors declare that they have no conflicts of interest.

Authors' Contributions

Conceptualization: Anish M.; Methodology: Jayaprakash V.; Software: Nivin Joy; Formal analysis and investigation: Jayaprabakar J.; Datacuration: Anish M.; Writing—original draft preparation: Anish M.; Writing—review and editing: Bency P.; Visualization: Sahaya Susmi S. K., Arunkumar T.; Supervision: Anish M.; Project administration: Jayaprakash V.

Acknowledgments

The Sathyabama Institute of Science and Technology provided financial assistance for this research. The authors would like to express their gratitude to the Center of Research for their generosity.

References

[1] Intel, "Thermal and Mechanical Design Guidelines," 2007.

[2] M. Rafati, "Application of nanofluids in computer cooling systems," in *Chemical Engineering*, University of Tehran, Tehran, 2010.

[3] D. B. Tuckerman and R. F. Pease, "High performance heat sinking for VLSI," *IEEE Electron Device Letters*, vol. 2, no. 5, pp. 126–129, 1981.

[4] A. K. Tiwari, N. S. Pandya, Z. Said, H. F. Öztop, and N. Abu-Hamdeh, "4S consideration (synthesis, sonication, surfactant, stability) for the thermal conductivity of CeO_2 with MWCNT and water based hybrid nanofluid: an experimental assessment," *Colloids and Surfaces A: Physicochemical and Engineering Aspects*, vol. 610, Article ID 125918, 2021.

[5] J. Lee and I. Mudawar, "Assessment of the effectiveness of nanofluids for single-phase and two-phase heat transfer in micro-channels," *Internatinal Journal of Heat and Mass Transfer*, vol. 50, no. 3–4, pp. 452–463, 2007.

[6] S. U. Choi and J. Eastman, *Enhancing Thermal Conductivity of Fluids with Nanoparticles*, Argonne National Laboratory, IL, USA, 1995.

[7] M. Rafati, A. Hamidi, and M. Shariati Niaser, "Application of nanofluids in computer cooling systems (heat transfer performance of nanofluids)," *Applied Thermal Engineering*, vol. 45–46, pp. 9–14, 2012.

[8] M. Korpyś, M. Al-Rashed, G. Dzido, and J. Wójcik, "CPU heat sink cooled by nanofluids and water: Experimental and numerical study," *Computer Aided Chemical Engineering*, vol. 32, pp. 409–414, 2013.

[9] L.-Y. Jeng and T.-P. Teng, "Performance evaluation of a hybrid cooling system for electronic chips," *Experimental Thermal and Fluid Science*, vol. 45, pp. 155–162, 2013.

[10] T. Yousefi, S. A. Mousavi, B. Farahbakhsh, and M. Z. Saghir, "Experimental investigation on the performance of CPU coolers: effect of heat pipe inclination angle and the use of nanofluids," *Microelectronics Reliability*, vol. 53, no. 12, pp. 1954–1961, 2013.

[11] P. Selvakumar and S. Suresh, "Convective performance of CuO/water nanofluid in an electronic heat sink," *Experimental Thermal and Fluid Science*, vol. 40, pp. 57–63, 2012.

[12] Z. Said, L. Syam Sundar, A. K. Tiwari et al., "Recent advances on the fundamental physical phenomena behind stability, dynamic motion, thermophysical properties, heat transport, applications, and challenges of nanofluids," *Physics Reports*, vol. 946, pp. 1–94, 2022.

[13] A. Kumar, P. R. Gupta, A. K. Tiwari, and Z. Said, "Performance evaluation of small scale solar organic Rankine cycle using MWCNT + R141b nanorefrigerant," *Energy Conversion and Management*, vol. 260, Article ID 115631, 2022.

[14] V. Kumar, A. Pare, A. K. Tiwari, and S. K. Ghosh, "Efficacy evaluation of oxide-MWCNT water hybrid nanofluids: an experimental and artificial neural network approach," *Colloids and Surfaces A: Physicochemical and Engineering Aspects*, vol. 620, Article ID 126562, 2021.

[15] O. Khonsue, "Experimental on the liquid cooling system with thermoelectric for personal computer," *Heat and Mass Transfer*, vol. 48, pp. 1767–1771, 2012.

[16] N. Tran, C. Zhang, T. Dang, and J.-T. Teng, "Numerical and experimental studies on pressure drop and performance index of an aluminum microchannel heat sink," in *Proceedings of the 2012 International Symposium on Computer, Consumer and Control*, pp. 252–257, Taichung, Taiwan, June 2012.

[17] D. D. Ma, G. D. Xia, J. Wang, Y. C. Yang, Y. T. Jia, and L. X. Zong, "An experimental study on hydrothermal performance of microchannel heat sinks with 4-ports and offset zigzag channels," *Energy Conversion and Management*, vol. 152, pp. 157–165, 2017.

[18] A. Ijam and R. Saidur, "Nanofluid as a coolant for electronic devices (cooling of electronic devices)," *Applied Thermal Engineering*, vol. 32, pp. 76–82, 2012.

[19] N. Putra, Yanuar, and F. N. Iskandar, "Application of nanofluids to a heat pipe liquid-block and the thermoelectric cooling of electronic equipment," *Experimental Thermal and Fluid Science*, vol. 35, no. 7, pp. 1274–1281, 2011.

[20] C. J. Ho, L. C. Wei, and Z. W. Li, "An experimental investigation of forced convective cooling performance of a microchannel heat sink with Al_2O_3/water nanofluid," *Applied Thermal Engineering*, vol. 30, no. 2–3, pp. 96–103, 2010.

[21] M. Kalteh, A. Abbassi, M. Saffar-Avval, A. Frijns, A. Darhuber, and J. Harting, "Experimental and numerical investigation of nanofluid forced convection inside a wide microchannel heat sink," *Applied Thermal Engineering*, vol. 36, pp. 260–268, 2012.

[22] J. A. Eastman, U. S. Choi, S. Li, L. J. Thompson, and S. Lee, "Enhanced thermal conductivity through the development of nanofluids," *MRS Online Proceedings Library*, vol. 457, pp. 3–11, 1996.

[23] C. T. Nguyen, G. Roy, C. Gauthier, and N. Galanis, "Heat transfer enhancement using Al_2O_3–water nanofluid for an electronic liquid cooling system," *Applied Thermal Engineering*, vol. 27, no. 8–9, pp. 1501–1506, 2007.

[24] D. Wen and Y. Ding, "Experimental investigation into convective heat transfer of nanofluids at the entrance region under laminar flow conditions," *International Journal of Heat and Mass Transfer*, vol. 47, no. 24, pp. 5181–5188, 2004.

[25] R. Nandha Kumar and D. Senthil Kumar, "An experimental investigation on thermal performance of nanofluids in a mini-channel heat sink," *Journal of Advances in Chemistry*, vol. 12, pp. 5152–5162, 2016.

[26] J. Jeong, C. Li, Y. Kwon, J. Lee, S. H. Kim, and R. Yun, "Particle shape effect on the viscosity and thermal conductivity of ZnO nanofluids," *International Journal of Refrigeration*, vol. 36, no. 8, pp. 2233–2241, 2013.

[27] S. Lee, S. U. Choi, S. Li, and J. Eastman, "Measuring thermal conductivity of fluids containing oxide nanoparticles," *Journal of Heat Transfer*, vol. 121, no. 2, pp. 280–289, 1999.

[28] J. A. Eastman, S. U. S. Choi, S. Li, W. Yu, and L. J. Thompson, "Anomalously increased effective thermal conductivities of ethylene glycol-based nanofluids containing copper nanoparticles," *Applied Physics Letters*, vol. 78, no. 6, pp. 718–720, 2001.

[29] P. K. Namburu, D. K. Das, K. M. Tanguturi, and R. S. Vajjha, "Numerical study of turbulent flow and heat transfer characteristics of nanofluids considering variable properties," *International Journal of Thermal Science*, vol. 48, no. 2, pp. 290–302, 2009.

[30] O. A. Alawi, N. A. C. Sidik, H. W. Xian, T. H. Kean, and S. N. Kazi, "Thermal conductivity and viscosity models of metallic oxides nanofluids," *International Journal of Heat and Mass Transfer*, vol. 116, pp. 1314–1325, 2018.

[31] K. A. Hamid, W. H. Azmi, R. Mamat, and K. V. Sharma, "Experimental investigation on heat transfer performance of TiO_2 nanofluids in water-ethylene glycol mixture," *International Journal of Heat and Mass Transfer*, vol. 73, pp. 16–24, 2016.

[32] B. Rimbault, C. T. Nguyen, and N. Galanis, "Experimental investigation of CuO–water nanofluid flow and heat transfer inside a microchannel heat sink," *International Journal of Thermal Science*, vol. 84, pp. 275–292, 2014.

[33] M. Nazari, M. Karami, and M. Ashouri, "Comparing the thermal performance of water, ethylene glycol, alumina and CNT nanofluids in CPU cooling: experimental study," *Experimental Thermal and Fluid Science*, vol. 57, pp. 371–377, 2014.

[34] A. Sivakumar, N. Alagumurthi, and T. Senthilvelan, "Effect of serpentine grooves on heat transfer characteristics of microchannel heat sink with different nanofluids," *Heat Transfer*, vol. 46, no. 3, pp. 201–217, 2017.

[35] M. Singh and R. Kumar, "Design and experimental analysis of rectangular wavy micro channel heat sink," *International Journal of Innovative Research in Advanced Engineering*, vol. 3, pp. 54–61, 2016.

[36] M. R. Thansekhar and C. Anbumeenakshi, "Experimental investigation of thermal performance of microchannel heat sink with nanofluids Al_2O_3/water and SiO_2/water," *Experimental Techniques*, vol. 41, pp. 399–406, 2017.

[37] E. Manay and B. Sahin, "Heat transfer and pressure drop of nanofluids in a microchannel heat sink," *Heat Transfer Engineering*, vol. 38, no. 5, pp. 510–522, 2017.

[38] M. Anbuvannan, M. Ramesh, G. Viruthagiri, N. Shanmugam, and N. Kannadasan, "*Anisochilus carnosus* leaf extract mediated synthesis of zinc oxide nanoparticles for antibacterial and photocatalytic activities," *Materials Science in Semiconductor Processing*, vol. 39, pp. 621–628, 2015.

[39] S. Vijayakumar, S. Mahadevan, P. Arulmozhi, S. Sriram, and P. K. Praseetha, "Green synthesis of zinc oxide nanoparticles using *Atalantia monophylla* leaf extracts: characterization and antimicrobial analysis," *Materials Science in Semiconductor Processing*, vol. 82, pp. 39–45, 2018.

[40] M. Hemmat Esfe, M. Afrand, A. Karimipour, W.-M. Yan, and N. Sina, "An experimental study on thermal conductivity of MgO nanoparticles suspended in a binary mixture of water and ethylene glycol," *International of Communications in Heat and Mass Transfer*, vol. 67, pp. 173–175, 2015.

[41] A. A. Alfaryjat, H. A. Mohammed, N. M. Adam, D. Stanciu, and A. Dobrovicescua, "Numerical investigation of heat transfer enhancement using various nanofluids in hexagonal microchannel heat sink," *Thermal Science and Engineering Progress*, vol. 5, pp. 252–262, 2018.

[42] Asus, 15 April 2019, https://www.asus.com/in.
[43] Intel, *Intel® Celeron® Dual-Core Processor, Thermal and Mechanical Design Guidelines*, Intel, Santa Clara, CA, USA, 2017.
[44] X. Wu, H. Wu, and P. Cheng, "Pressure drop and heat transfer of Al_2O_3–H_2O nanofluids through silicon microchannels," *Journal of Micromechanics and Microengineering*, vol. 19, Article ID 105020, 2009.
[45] R. L. Hamilton and O. K. Crosser, "Thermal conductivity of heterogeneous two-component systems," *Industrial & Engineering Chemistry Fundamentals*, vol. 1, no. 3, pp. 187–191, 1962.
[46] S. M. S. Murshed, K. C. Leong, and C. Yang, "Enhanced thermal conductivity of TiO_2—water based nanofluids," *International Journal of Thermal Sciences*, vol. 44, no. 4, pp. 367–373, 2005.
[47] W. Yu and S. U. S. Choi, "The role of interfacial layers in the enhanced thermal conductivity of nanofluids: a renovated Maxwell model," *Journal of Nanoparticle Research*, vol. 5, pp. 167–171, 2003.
[48] E. V. Timofeeva, A. N. Gavrilov, J. M. McCloskey et al., "Thermal conductivity and particle agglomeration in alumina nanofluids: experiment and theory," *Physical Review E*, vol. 76, no. 6, Article ID 061203, 2007.
[49] G. K. Batchelor, "The effect of Brownian motion on the bulk stress in a suspension of spherical particles," *Journal of Fluid Mechanics*, vol. 83, no. 1, pp. 97–117, 1977.
[50] D. A. Drew and S. L. Passman, "Theory of multicomponent fluids," *Applied Mathematical Sciences*, vol. 135, Springer, New York, NY, 1999.
[51] H. C. Brinkman, "The viscosity of concentrated suspensions and solutions," *The Journal of Chemical Physics*, vol. 20, no. 4, p. 571, 1952.
[52] X. Wang, X. Xu, and S. U. S. Choi, "Thermal conductivity of nanoparticles—fluid mixture," *Journal of Thermophysics and Heat Transfer*, vol. 13, no. 4, pp. 474–480, 1999.